

# A New Method for Cardiac Computed Tomography Regional Function Assessment

## Stretch Quantifier for Endocardial Engraved Zones (SQUEEZ)

Amir Pourmorteza, MSc; Karl H. Schuleri, MD; Daniel A. Herzka, PhD;  
Albert C. Lardo, PhD; Elliot R. McVeigh, PhD

**Background**—Quantitative assessment of regional myocardial function has important diagnostic implications in cardiac disease. Recent advances in CT imaging technology have allowed fine anatomic structures, such as endocardial trabeculae, to be resolved and potentially used as fiducial markers for tracking local wall deformations. We developed a method to detect and track such features on the endocardium to extract a metric that reflects local myocardial contraction.

**Methods and Results**—First-pass CT images and contrast-enhanced cardiovascular magnetic resonance images were acquired in 8 infarcted and 3 healthy pigs. We tracked the left ventricle wall motion by segmenting the blood from myocardium and calculating trajectories of the endocardial features seen on the blood cast. The relative motions of these surface features were used to represent the local contraction of the endocardial surface with a metric we call Stretch Quantifier of Endocardial Engraved Zones (SQUEEZ). The average SQUEEZ value and the rate of change in SQUEEZ were calculated for both infarcted and healthy myocardial regions. SQUEEZ showed a significant difference between infarct and remote regions ( $P < 0.0001$ ). No significant difference was observed between normal myocardium (noninfarcted hearts) and remote regions ( $P = 0.8$ ).

**Conclusions**—We present a new quantitative method for measuring regional cardiac function from high-resolution volumetric CT images, which can be acquired during angiography and myocardial perfusion scans. Quantified measures of regional cardiac mechanics in normal and abnormally contracting regions in infarcted hearts were shown to correspond well with noninfarcted and infarcted regions as detected by delayed enhancement cardiovascular magnetic resonance images. (*Circ Cardiovasc Imaging*. 2012;5:243-250.)

**Key Words:** four-dimensional computed tomography ■ cardiac imaging techniques ■ magnetic resonance imaging ■ ischemic heart disease ■ myocardial contraction ■ volumetric computed tomography

Coronary angiography is currently the most prevalent use of cardiac CT. In this study, we aimed to assess systolic regional cardiac function from high-resolution volumetric cardiac CT acquisitions, which can be acquired in conjunction with routine CT angiography. Assessment of regional myocardial function has value in the diagnosis and monitoring of myocardial ischemia and myocardial dyssynchrony.<sup>1,2</sup> Most mechanical analyses in the clinical setting is based on echocardiographic methods derived from 2D motion data. Not all tomographic imaging modalities are capable of producing data with adequate temporal and spatial resolution for detailed regional function assessment. One difficulty with quantitative tomographic methods to estimate myocardial function is the inability to obtain adequate landmarks in the heart because of poor spatial resolution.

### Clinical Perspective on p 250

Cardiovascular magnetic resonance (CMR) tissue tagging, which is currently considered the reference method, is validated and accurate, but it is slow, has poor resolution in the slice selection direction, and requires extended breath holding, and its image analysis is time consuming because of the manual segmentation required to detect the myocardial borders.<sup>3</sup> In addition, CMR imaging is still considered a contraindication in the rapidly growing population of patients with implanted pacemakers or implantable cardioverter-defibrillators.

Recent dramatic advances in cardiac CT imaging techniques allow for volumetric functional imaging of the entire heart with a few gantry rotations.<sup>3-9</sup> The high temporal resolution acquisitions of the entire cardiac volume with wide-range detector CT allows a contrast bolus to be imaged over a short window in the heart cycle with very high spatial

Received January 31, 2011; accepted February 14, 2012.

From the Department of Biomedical Engineering (A.P., D.A.H., A.C.L., E.R.M.) and Division of Cardiology (K.H.S., A.C.L.), Department of Medicine, Johns Hopkins University School of Medicine, Baltimore, MD.

Correspondence to Elliot R. McVeigh, PhD, 720 Rutland Ave, Ste 720 Ross Building, Baltimore, MD 21205. E-mail emcveigh@jhu.edu

© 2012 American Heart Association, Inc.

*Circ Cardiovasc Imaging* is available at <http://circimaging.ahajournals.org>

DOI: 10.1161/CIRCIMAGING.111.970061

resolution, making visible fine anatomic structures, such as trabeculae, on the endocardial surface. We took advantage of the resolution now available with wide-range detector CT to develop a method to detect and track the fine curvature-based geometric features on the endocardial surface, which are used to extract a metric that reflects the cardiac muscle contraction. It has been previously shown that differential geometry features of the myocardial surfaces can be used to estimate the motion field from 3D anatomic images<sup>10–12</sup>; however, the low spatial resolution of the images has been a limitation. Here, we evaluate the feasibility of tracking the left ventricular (LV) wall motion and assessing local cardiac function in high-resolution first-pass volumetric cardiac CT images using a fast, nonrigid, surface registration algorithm that matches geometric features of the surface over time.

## Methods

### Animal Model

All animal studies were approved by the Johns Hopkins University Institutional Animal Care and Use Committee and comply with the *Guide for the Care and Use of Laboratory Animals* (National Institutes of Health Publication no. 80–23, revised 1985).

Pigs with chronic myocardial infarctions (MIs) were created as previously described.<sup>13</sup> Briefly, MI was induced by engaging the left anterior descending coronary artery (LAD) with an 8F hockey stick catheter under fluoroscopic guidance. Then, a 0.014-in angioplasty guidewire was inserted into the LAD, and a 2.5×12-mm Maverick balloon (Boston Scientific) was inflated to 4 atm just distal to the second diagonal branch of the LAD. After 120 minutes, occlusion of the vessel was terminated by deflating the balloon, and restoration of flow in the LAD was confirmed by angiography. CT and MRI studies were performed ≈130 to 180 days after MI induction. A total of 11 animals were studied (7 chronic MI, 1 acute MI, and 3 healthy).

### CT Imaging

Each animal was scanned with electrocardiographic monitoring using a 0.5-mm×320-row detector scanner (Aquilion ONE; Toshiba Medical Systems Corporation). Animals received intravenous metoprolol (2–5 mg), amiodarone (50–150 mg), or both to achieve a heart rate of <100 beats/min. After scout acquisition, a 50- to 60-mL bolus of iodixanol (320 mg iodine/mL; Visipaque; Amersham Health) was injected intravenously, and a first-pass cardiac perfusion scan for the entire cardiac cycle was performed. During CT acquisition, respiration was suspended, and imaging was performed using a retrospectively gated CT protocol with the following parameters: gantry rotation time, 350 ms; temporal resolution, up to 58 ms using multisegment reconstruction<sup>9</sup>; detector collimation, 0.5 mm×320 rows (isotropic voxels, 0.5×0.5×0.5 mm<sup>3</sup>); tube voltage, 120 kV; and tube current, 400 mA. One infarcted data set was acquired using x-ray tube current modulation of 10% of the maximum, with the maximum current at only the 75% time point of the R-R interval. Images were reconstructed at every 10% of the R-R interval in systole using a standard kernel (FC03), QDS+ noise reduction filter, and a multisegment (3–5 beats) reconstruction algorithm. Electrocardiographic editing to account for arrhythmias was performed when necessary. In addition, a set of low-dose, prospectively gated scans (120 kV and 20 mA at 0% and 50% of R-R) along with a high-dose (120 kV and 400 mA) retrospectively gated scan were acquired for 1 animal to assess the feasibility of tube current reduction and prospective gating for cardiac function analysis.

### Cardiovascular Magnetic Resonance

In vivo CMR images were acquired using a 3T MR scanner (Achieva; Philips) with a 32-element cardiac phased array. Myocardial viability was visualized using late gadolinium enhancement images acquired 20 to 25 minutes after intravenous injection of a

double dose of gadolinium diethylenetriaminepentaacetic acid (0.2 mmol/kg body weight) (Magnevist; Berlex). A 3D, ECG-triggered, independent respiratory navigator-gated, breath-hold, phase-sensitive inversion recovery gradient echo imaging pulse sequence was used.<sup>14</sup> Imaging field of view was 24×24×12 cm<sup>3</sup>, with an imaging matrix of 200×195×30, yielding an acquired voxel size of 1.20×1.23×4.0 mm<sup>3</sup> reconstructed to 0.91×0.91×2.0 mm<sup>3</sup>. Other relevant imaging parameters were as follows: flip angle, 15°; repetition time, 5.3 ms; echo time, 2.6 ms; and receiver bandwidth, 289 Hz/pixel.

### Image Analysis

For each systolic cardiac phase, the blood in the LV was segmented from the myocardium by thresholding the voxel intensities roughly between 200 and 650 Hounsfield units. After manually pruning the coronaries; aorta; and, in some data sets, the right ventricle (using the Medical Image Processing, Analysis, and Visualization program available from the National Institutes of Health at <http://mipav.cit.nih.gov>), a triangulated mesh representing the endocardial surface was extracted from the boundary surface of the LV blood cast (Figure 1A–1C and 1E). All computations, unless specified otherwise, were done using Matlab (MathWorks Inc) software. To compare the results of the proposed algorithm to existing CT wall motion tracking software, the data sets were analyzed using Vitrea FX software (Vital Images).

### Motion Tracking

We tracked the LV wall motion by calculating trajectories for the points on the endocardial mesh. Each endocardial surface was represented by a triangular mesh. To track the points on the meshes from end diastole (ED) to end systole (ES), the surfaces needed to have the same number of triangles, with a 1:1 correspondence between the vertices. This was accomplished by choosing a template mesh (in this case, the ED mesh) and warping it onto a target mesh (any systolic mesh, eg, the ES mesh) such that every triangle on the template mesh had a corresponding triangle on the target mesh (Figure 1D and 1E). We chose a nonrigid point registration algorithm termed *coherent point drift* (CPD) for surface warping. CPD is a probabilistic method used for nonrigid surface registration in which surface points are forced to move coherently as a group to preserve the topological structure of the point sets.<sup>15</sup> The coherence constraint was imposed by regularizing the displacement field and using variational calculus to derive the optimal warping. A fast implementation of CPD, based on the fast Gaussian transform, was used to reduce the massive computational burden associated with high-resolution CT data.

To match the anatomy through surface warping, the homologous anatomic features and their correspondences needed to be identified. Therefore, features engraved on the endocardial surface by fine anatomic structures, such as trabeculae and papillary muscles, were encoded using a scale-independent local shape measure termed *shape index* (SI) (Figures 1D and 2) and incorporated in the warping algorithm to further improve its accuracy. The SI is a curvature-based measure, and for each point is defined by

$$(1) \quad SI = \frac{2}{\pi} \arctan \frac{k_1 + k_2}{k_1 - k_2}$$

where  $k_1$  and  $k_2$  are the principal (signed maximum and minimum) curvatures at that point. Figure 2 shows SI values for different surface shapes. For a saddle point,  $k_1 = -k_2$ ; thus,  $SI = 0$ . For a spherical surface,  $k_1 = k_2 \neq 0$ , and the  $SI = -1$  if curvatures are negative and  $+1$  if they are positive, corresponding to a spherical cup and cap, respectively. For a valley,  $k_1 = 0$ , and  $k_2$  can have any negative value (by definition  $k_1 \geq k_2$ ); thus, as long as  $k_2$  is nonzero we have:

$$SI = \frac{2}{\pi} \arctan \frac{+k_2}{-k_2} = -0.5$$

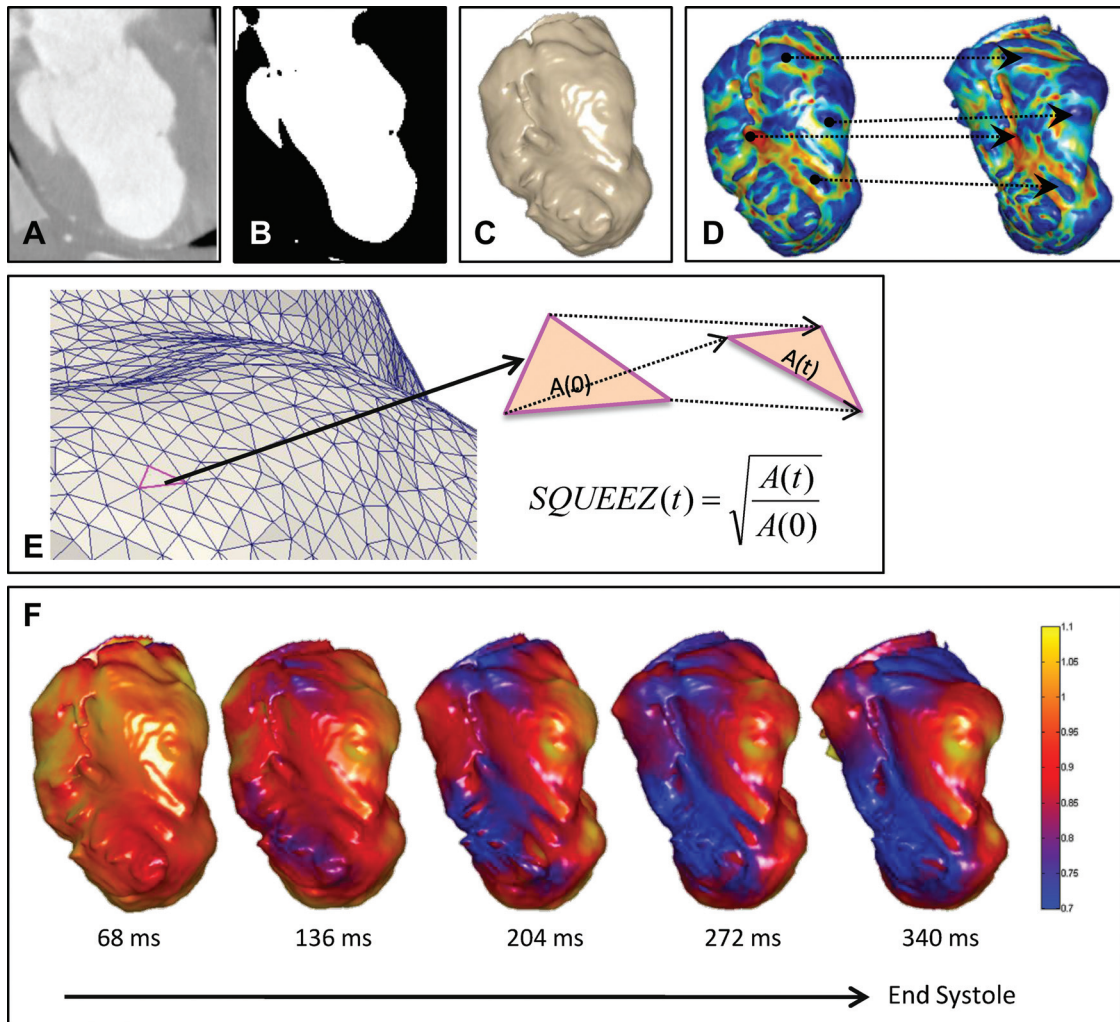


**Figure 1.** Steps of the proposed method. **A**, Cropped axial CT image of the left ventricle. **B**, The blood pool segmented from the volume by thresholding. **C**, Endocardial surface extracted from the segmented images (inferolateral wall facing viewer). **D** Shape index values calculated to encode the features engraved by the trabecular structures on the endocardial surface. Coherent point drift algorithm is used to find the correspondence between the endocardial features at end diastole (ED) (left), used as template, and other systolic phases (right), used as targets. **E**, Coherent point drift warping results in endocardial meshes with corresponding triangles. A measure of regional cardiac function, called SQUEEZ, is calculated for each triangle on the ED endocardial surface mesh by tracking the corresponding triangle at different cardiac phases.  $A(0)$  is the area of the triangle at ED, and  $A(t)$  is its area at cardiac phase  $t$ . SQUEEZ is the square root of the ratio of the area of a triangle on the endocardial surface at a systolic phase to its area at ED. **F**, SQUEEZ maps calculated for every triangle on the endocardial surface at 5 cardiac phases from ED to end systole. SQUEEZ indicates Stretch Quantifier for Endocardial Engraved Zones.

The same argument holds for a ridge, which will have an SI value of 0.5. The intermediate SI values correspond to when these shapes are smoothly warped to each other.<sup>16,17</sup>

An important property of SI is that it is stretch invariant. As mentioned previously, surface features (eg, ridges and valleys) will have a certain SI value solely based on their shape and not on their curvatures (ie, steepness). Therefore, as long as the topology of the surface does not change under compression or stretch, the anatomic features, such as ridges and valleys on the endocardial surface, will retain their SI values. This property makes SI a useful tool for encoding endocardial features.

The output of the CPD algorithm is a displacement field that is used to calculate measures of local cardiac function. We propose a measure of local cardiac function called Stretch Quantifier of Endocardial Engraved Zones (SQUEEZ), which is defined as follows:

$$(2) \quad SQUEEZ(v, t) = \sqrt{\frac{A(v, t)}{A(v, 0)}}$$

where  $A(v, 0)$  is the area of the small triangular patch ( $v$ ) on the endocardial mesh at ED, and  $A(v, t)$  is the area of the same patch at time  $t$ . SQUEEZ is calculated for each triangular patch on the surface, resulting in a high-resolution local cardiac function map of the LV.

### Statistical Analysis

For the data pool obtained from the 11 animals, 2-tailed paired Student  $t$  test statistical analyses were performed on the SQUEEZ value and the slope of SQUEEZ versus time to assess the difference in the means of these parameters in healthy and infarcted regions. The accuracy of the registration algorithm was evaluated using the mean of the minimum pairwise Euclidean distance between the target and the warped data sets (ie, for each point on the template mesh, the Euclidean distance to every point on the warped mesh is calculated, and the minimum is chosen). The mean  $\pm$ SD of the minimum distances is reported.

### Results

To evaluate resting LV function, the blood pool of the LV was segmented in the ED and ES phases in the 3D volume

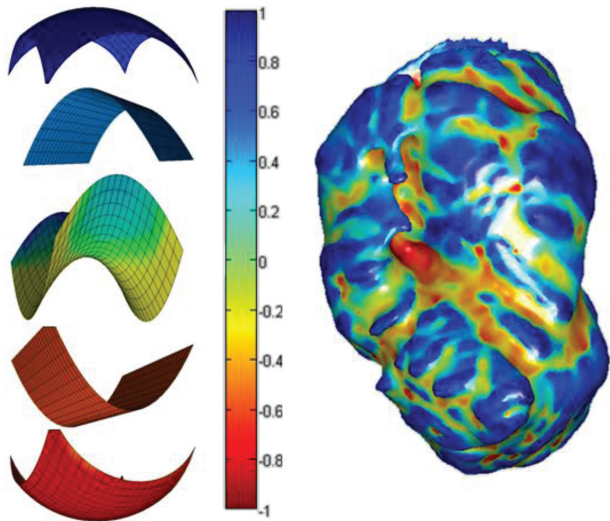


**Figure 2.** Local shape encoding using shape index (SI). SI values for the point at the center of the simple surfaces (left), including from top to bottom, spherical cap, ridge, saddle point, valley, and spherical cup. For the spherical cap,  $k_1=k_2>0$ ; thus,  $SI=+1$ . For the ridge,  $k_1>0$ ,  $k_2=0$ , and  $SI=+0.5$ . For the saddle point,  $k_1=-k_2\neq 0$ , and  $SI=0$ . For the valley,  $k_1=0$  and  $k_2<0$ ; thus,  $SI=-0.5$ . For the spherical cup,  $k_1=k_2<0$  results in  $SI=-1$ . Other SI values are caused by smooth deformation of these surfaces. An example of SI calculated for an end-diastole endocardial surface is shown on the right.

and ED volume, ES volume, stroke volume, and ejection fraction were calculated for the LV (Figure 3). SQUEEZ values were measured in healthy and infarcted animals at different cardiac phases (Figure 4) and different locations of infarcted and remote myocardium as detected by contrast-enhanced MRI (Figure 5).

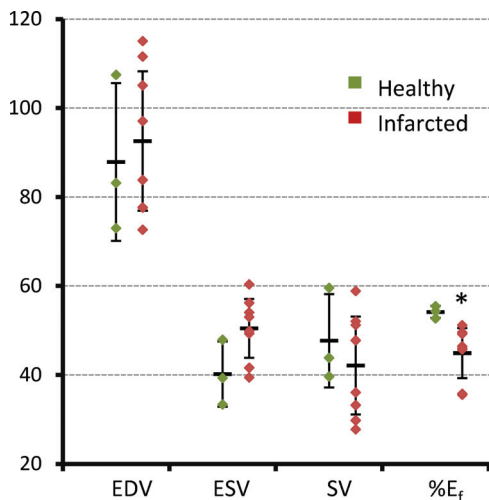


**Figure 3.** Global left ventricle function measures for healthy (n=3) and infarcted (n=8) pigs. For healthy versus infarcted pigs, respectively, EDV is  $87.8\pm 17.7$  versus  $92.5\pm 15.6$  mL; ESV,  $40.1\pm 7.3$  versus  $50.4\pm 6.6$  mL; SV (EDV–ESV),  $47.6\pm 10.5$  versus  $42.0\pm 11.0$  mL; and  $\%E_f$  (SV/EDV),  $54.1\pm 1.3\%$  versus  $44.9\pm 5.6\%$ . The bars and whiskers indicate the mean  $\pm$  SD of the quantities, respectively. EDV indicates end-diastolic volume; E<sub>f</sub>, ejection fraction; ESV, end-systolic volume; SV, stroke volume. \* $P<0.05$ .

### Accuracy of the Nonrigid Registration Algorithm (CPD)

The accuracy of the nonrigid registration algorithm was evaluated using the mean of the minimum Euclidean distance between the target and warped surfaces evaluated at all points. Over the 11 animals analyzed by our method, there was a subpixel average error of  $0.6\pm 0.4$  pixels ( $0.3\pm 0.2$  mm). All the triangular patches on the meshes had sides  $\geq 1$  pixel.

### Regional Cardiac Function

SQUEEZ was calculated for every point on the LV endocardial surface at each cardiac phase. All infarcted animals showed abnormal stretching in the LAD territory, which was consistent with the infarct model used in this work. One animal showed 2 distinct MI zones, and this was confirmed by examining the CMR image, which showed a secondary MI in the inferior wall.

Figure 4 shows SQUEEZ bull’s-eye plots calculated for 5 consecutive phases from ED to ES. Areas in yellow (SQUEEZ >1) show abnormal stretch because of MI.

Contrast-enhanced CMR images were used as the gold standard to verify the location of the infarcted regions detected in SQUEEZ maps (Figure 5A). Points were selected on regions of the endocardial surface near the MI zones as defined by the contrast-enhanced CMR images. Approximately the same number of points were selected in a remote region of the heart with no sign of MI (Figure 5B). The size of the selected regions roughly corresponded to that of 1 LV segment in the 17-segment American Heart Association model.<sup>18</sup>

The average SQUEEZ value was calculated for each zone and showed a significant difference ( $P<0.0001$ ) between MI and non-MI regions in infarcted animals (Figure 5B). For healthy animals, a region on the lateral wall was chosen corresponding to the remote non-MI region selected in infarcted animals. The SQUEEZ values for the non-MI region in the infarcted hearts and the regions chosen in the healthy hearts were not significantly different.

In addition to SQUEEZ, the rate of change in SQUEEZ also showed a significant difference ( $P<0.0001$ ) between MI and non-MI regions in the infarcted animals (Figure 5C), and no difference was found between the same lateral regions in healthy and non-MI regions. Non-MI regions showed an average SQUEEZ rate of  $\approx -0.6\pm 0.2$ , whereas the MI zones had a rate of  $\approx 0\pm 0.1$ , showing little or no stretch or contraction.

The SQUEEZ time plots for the tube current modulated data set showed higher SDs because of increased noise levels. However, the difference between MI and non-MI regions was still significant, and the trend of the plots were similar to those of the high-dose data sets (Figure 5B).

The SQUEEZ map was calculated for the low-dose prospectively gated data set and compared to the SQUEEZ of the high-dose retrospectively gated data set at 50% of the R-R interval. The difference between the SQUEEZ maps was computed (Figure 6). The results show low bias (0.01; 95% CI,  $-0.12$  to  $0.15$ ) between the high-dose retrospective and the low-dose prospective scans. The differences could be

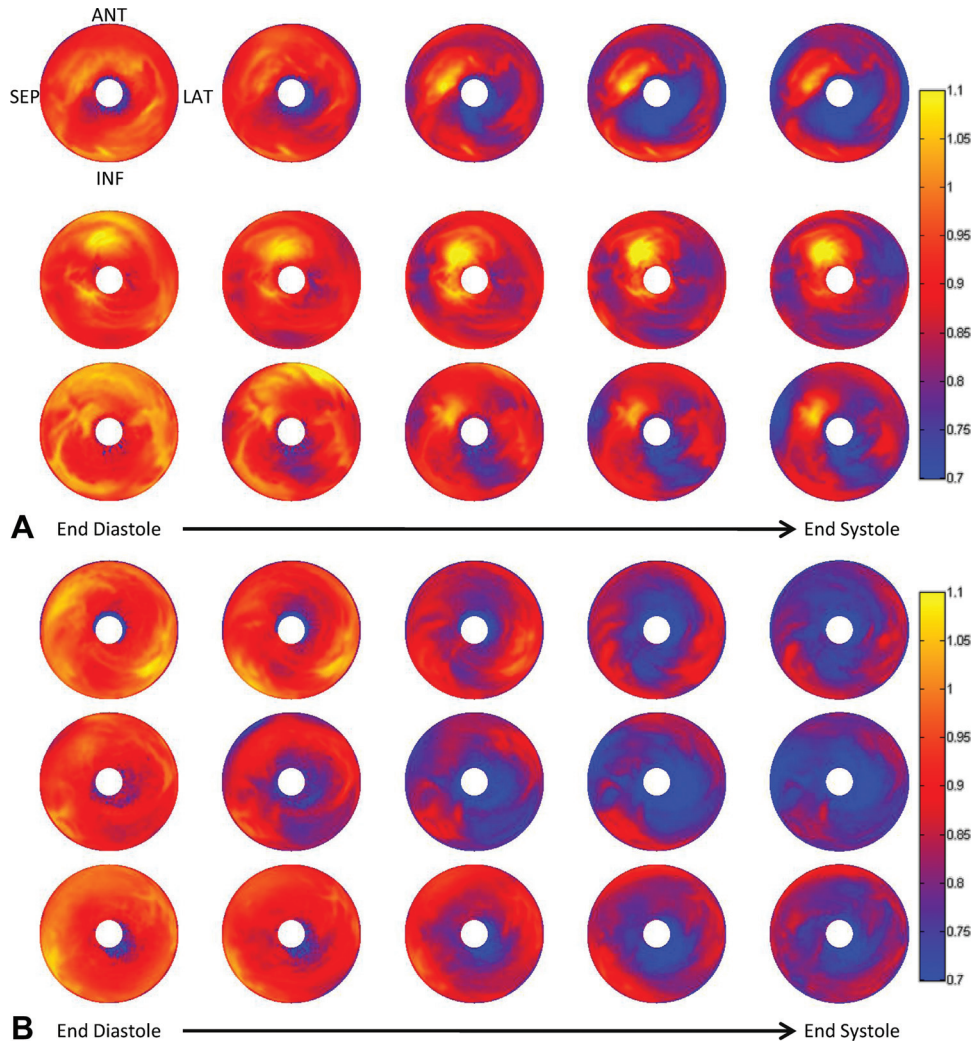


**Figure 4.** Bull's-eye plots of the SQUEEZ values for 3 typical infarcted (A) and 3 healthy animals (B) from end diastole to end systole at 10% R-R intervals. Infarcted animals show abnormal stretching of the endocardium in LAD coronary artery territory (anterior and anteroseptal segments), which is consistent with the infarction model (LAD coronary artery occlusion after the second diagonal) used in this study. SQUEEZ indicates Stretch Quantifier for Endocardial Engraved Zones; LAD, left anterior descending.

attributed not only to the increased noise due to lower tube current, but also to heart rate variations among the acquisitions. More experiments are going to be carried out to fully investigate the effects of CT noise on the accuracy of SQUEEZ. Use of the low-dose prospective scan decreased the radiation dose by  $\approx 10$ -fold. The low bias and 95% CI of the low-dose scan make the use of low-dose, prospectively gated CT for cardiac function very promising.

Regional ejection fraction (rEF) was calculated at ES for each cardiac segment using Vitrea fX software. The automatic segmentation of endocardial borders required manual correction, which took  $\approx 150 \pm 15$  minutes, as opposed to  $4 \pm 2$  minutes of operator interaction required in the proposed method. SQUEEZ values were averaged into the American Heart Association 16 segments and compared to 1-rEF values obtained from Vitrea fX. There was good correlation ( $r=0.81, P<0.001$ ) for the 6 midcavity segments (segments 7–12), but no correlation was found in basal and apical segments in any of the data sets.

### Discussion

We have developed a new method for measuring regional cardiac function with high resolution from volumetric CT acquisitions that has proven to be effective in quantifying regional cardiac mechanics and detecting infarcted regions in a large animal model. Volumetric CT data used in this work can be reconstructed from the routine dose-modulated coronary angiography CT scans. The method also eliminates the laborious human interaction required to segment the cardiac data for functional analysis that has plagued cardiac imaging for the past 2 decades.

Current methods for CT regional cardiac function analysis involve time-consuming manual segmentation or manual correction of segmentation of the myocardium. These methods generally apply smooth contours to delineate epicardial and endocardial boundaries, thus failing to capture the fine anatomic endocardial structures visible in wide-range detector CT that can be used as landmarks to guide the motion tracking algorithm. Furthermore, these algorithms normally

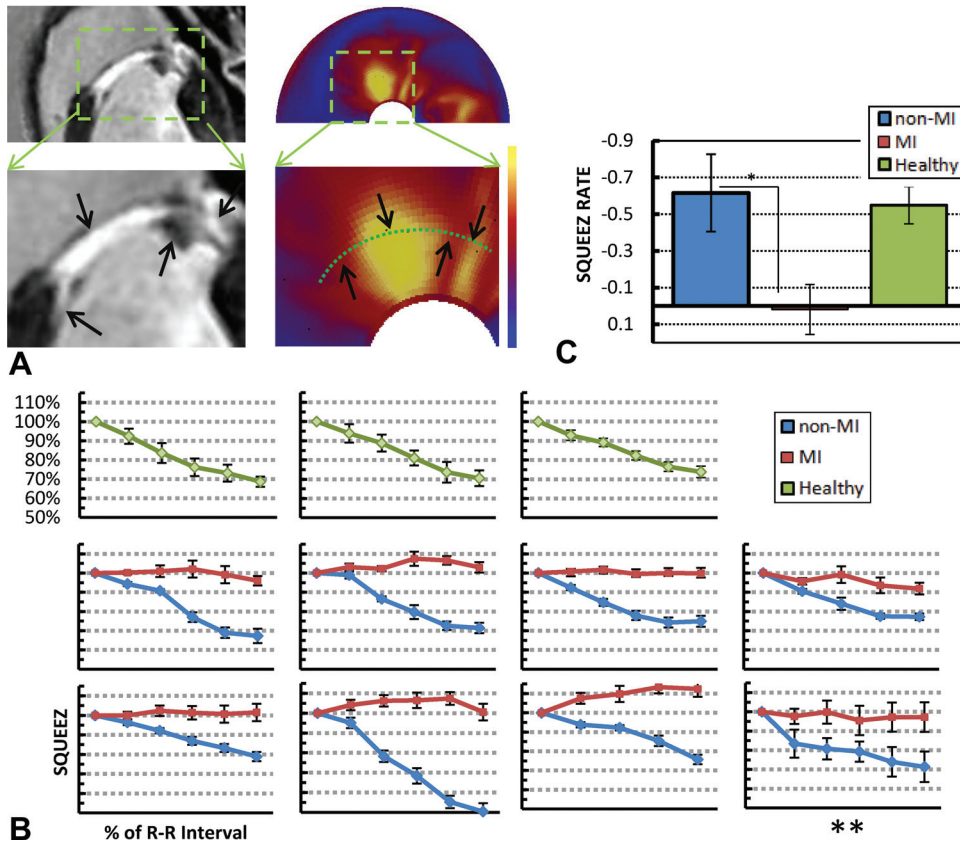


**Figure 5.** **A**, A short-axis phase-sensitive inverted recovery MRI of an animal with an anterior/anteroseptal heterogeneously infarcted region (left). The infarcted region has characteristic high signal intensity. End-systolic SQUEEZ bull's-eye plot of the same animal (right). The short-axis image on the left approximately corresponds to the SQUEEZ values along the dashed arc. The infarcted subregions in the MRI correspond to the regions detected in the SQUEEZ plot, depicted by the arrows. Shown from left to right is a section with some loss of function, a section with complete loss of function that shows wall expansion, a small section with some contractility, and a fourth subregion with loss of function. **B**, Time plots of the average SQUEEZ values for healthy, MI, and non-MI regions in systole for 3 healthy and 7 infarcted pigs. The regions were chosen to be roughly the size of segments in the American Heart Association 17-segment model. All infarcted pigs showed significant differences in SQUEEZ for MI and non-MI regions ( $P < 0.0001$ ). \*\*Dose-modulated data set. **C**, Average SQUEEZ rate values calculated by averaging over the slopes of lines fitted to the curves in **B**. SQUEEZ rate is significantly different between MI and non-MI regions in infarcted hearts ( $P < 0.0001$ ). There was no significant difference between non-MI regions in the infarcted hearts and the same regions chosen in the healthy hearts. MI indicates myocardial infarction; SQUEEZ, Stretch Quantifier for Endocardial Engraved Zones.

track the 3D motion by analyzing the displacements in stacks of 2D slices (usually oriented in the short axis). The longitudinal displacement of tissue into and out of a short-axis slice can appear to be a change in the myocardial wall

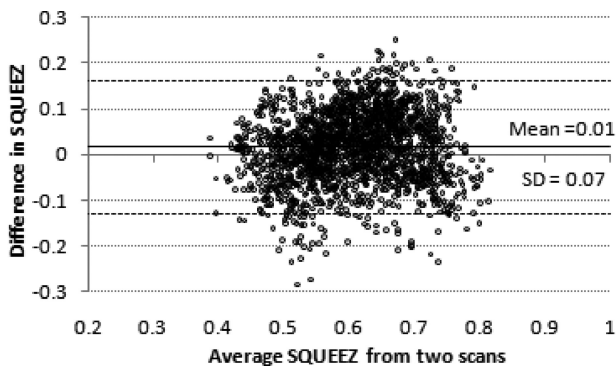


**Figure 6.** Sample comparison between high-dose and low-dose scans. Bland-Altman plot of the SQUEEZ values calculated from high-dose retrospective and low-dose prospective scans shows low bias (mean,  $0.01 \pm 0.07$ ). Dashed lines denote 95% CI ( $-0.12$  to  $0.15$ ) ( $N = 2250$  SQUEEZ estimates).

thickness in that short-axis slice, but it is in fact just bulk displacement of tissues in 3D space. This artifact is more prominent in basal and apical segments in which the position of the short-axis contours may change significantly because of through-plane motion. This could explain the poor correlation between rEF and SQUEEZ in apical and basal segments. In addition, rEF calculation is based on distance from a centerline: If the centerline is not chosen correctly, there will be large errors in rEF calculations. This artifact is more prominent in apical slices, where a small change in the position of the centerline could result in large rEF values. Although the centerlines were chosen carefully, the irregular shape of the endocardial contour in apical slices, especially in hearts that have undergone significant LV remodeling, would still cause very large rEF values in some data sets.

### Comparison With Other Modalities

Echocardiography is widely used in clinics for cardiac function and dyssynchrony analysis but does not produce a detailed map of the coronaries and is limited by the available acoustic window. Although echocardiography has very high

temporal resolution, the available window for transducer placement limits the orientation of the imaging plane. Furthermore, the variance of repeated echocardiographic measures is fairly high because of dependence on operator experience, machine settings, available acoustic windows, and angle of incidence effects.

CMR is another highly attractive modality for regional cardiac function analysis. However, this method also has some practical drawbacks, including higher cost, occasional gating failures, more-complex scanning protocols, and longer scanning times. The inability to study the growing population of patients with implanted electronic devices, which is especially relevant in patients with previous MI is another drawback. With its high isotropic resolution, CT decreases partial volume effects, accurately characterizes the blood-myocardium interface, and eliminates through-plane motion artifacts.

### Radiation and Iodinated Contrast

Radiation exposure and iodinated contrast agent dose are still primary concerns with the increasing use of CT technology in diagnostic cardiac imaging and have become a centerpiece of new hardware, software, and imaging protocol improvements. Wide-range detector CT, with full cardiac coverage, does not need an overlapping radiation exposure and long scan times, as required in traditional helical CT imaging systems and, thus, provides a significant radiation and contrast dose savings for cardiac imaging.<sup>8,19</sup> Significant leaps have been made in the dose reduction algorithms parallel to advances in hardware in the past couple of years. Furthermore, we extended our validations to tube current modulation of 10% and prospectively gated scans<sup>8</sup> with tube currents as low as 5% of the high-dose scans, and the initial results were encouraging and confirmed the feasibility of using low-dose CT.

Iterative reconstruction algorithms<sup>20–22</sup> could potentially improve the results of our method further; however, they were not available at the time of these measurements. When available, these algorithms and numerous CT image noise reduction methods<sup>23,24</sup> are expected to improve the results of SQUEEZ by reducing the noise at current x-ray tube settings or reducing dose with tube current reduction. In the present study, we demonstrated that SQUEEZ is capable of quantifying regional cardiac function with routine CT acquisitions; determination of the minimum number of photons for clinically acceptable images requires further investigation.

### Study Limitations

Wide-range detector CT has limitations in temporal resolution intrinsic to CT imaging. This limitation has been reduced, with improvements in multibeam segmented image reconstruction and gantry rotation speed such that temporal resolution of <60 ms is now achievable.<sup>9</sup> Although it is possible to calculate SQUEEZ from single-beat CT acquisitions, especially during systole, multibeam reconstructions will produce more-robust SQUEEZ values with higher temporal resolution.

The reliance on SQUEEZ alone, rather than strain measures, such as myocardial shortening, to characterize local function may be a limitation. Although SQUEEZ and myo-

cardial strain both reflect mechanical contractile function of the heart, a simple mathematical relation between MRI midwall strain and SQUEEZ may not be found because they measure 2 different physical parameters. Strain measures shortening in the myocardium and is most reliable in the midwall because of partial volume artifacts near the epicardial and endocardial borders in MRI. SQUEEZ, on the other hand, reflects endocardial deformation by measuring local changes in the area of the endocardial surface. Endocardial deformation metrics like SQUEEZ have an advantage in detecting the myocardial ischemic cascade and the resulting transmural strain gradient.<sup>25</sup> A recent study has shown that a significant correlation exists between surface deformation and 1D strain metrics in 3D speckle-tracking images.<sup>26</sup> These results lead us to believe that there will be a linear relationship between SQUEEZ and strain metrics, but we have yet to determine the precise relationship between SQUEEZ and circumferential shortening under all circumstances. Although the data obtained in this study are promising, larger studies are needed to establish the precise diagnostic accuracy of SQUEEZ.

### Acknowledgments

We thank Kristine Evers, Valeria Sena-Weltin, Jorge Guzman, and Theresa Caton for their assistance with animal preparation, CT acquisition, and data management.

### Sources of Funding

Funding for animal preparation was provided by National Institutes of Health grants R01-HL64795 and R01-HL094610 (Henry Halperin, principal investigator). A stipend for Mr Pourmorteza was partially provided by a Siemens PhD fellowship for imaging research.

### Disclosures

Dr McVeigh has ownership interest in MRI Interventions Inc. Dr McVeigh has intellectual property in the field (US Patent 6,171,241, January 9, 2001 for the method for measuring myocardial motion and the like, E. R. McVeigh and B. D. Bolster).

### References

- Lardo AC, Abraham TP, Kass DA. Magnetic resonance imaging assessment of ventricular dyssynchrony: current and emerging concepts. *J Am Coll Cardiol*. 2005;46:2223–2228.
- Helm RH, Leclercq C, Faris OP, Ozturk C, McVeigh E, Lardo AC, Kass DA. Cardiac dyssynchrony analysis using circumferential versus longitudinal strain: implications for assessing cardiac resynchronization. *Circulation*. 2005;111:2760–2767.
- McVeigh E. Regional myocardial function. *Cardiology Clinics*. 1998;16:189–206.
- Rybicki F, Otero H, Steigner M, Vorobiof G, Nallamshetty L, Mitsouras D, Ersoy H, Mather R, Judy P, Cai T, Coyner K, Schultz K, Whitmore A, Di Carli M. Initial evaluation of coronary images from 320-detector row computed tomography. *Int J Cardiovasc Imaging*. 2008;24:535–546.
- Steigner M, Otero H, Cai T, Mitsouras D, Nallamshetty L, Whitmore A, Ersoy H, Levit N, Di Carli M, Rybicki F. Narrowing the phase window width in prospectively ECG-gated single heart beat 320-detector row coronary CT angiography. *Int J Cardiovasc Imaging*. 2009;25:85–90.
- Choi SI, George RT, Schuleri KH, Chun EJ, Lima JAC, Lardo AC. Recent developments in wide-detector cardiac computed tomography. *Int J Cardiovasc Imaging*. 2009;25:23–29.
- George R, Lardo A, Lima J. Added value of CT myocardial perfusion imaging. *Curr Cardiovasc Imaging Rep*. 2008;1:96–104.
- Kitagawa K, Lardo AC, Lima JAC, George RT. Prospective ECG-gated 320 row detector computed tomography: implications for CT angiography and perfusion imaging. *Int J Cardiovasc Imaging*. 2009;25:201–208.

9. Schuleri KH, George RT, Lardo AC. Applications of cardiac multidetector CT beyond coronary angiography. *Nat Rev Cardiol*. 2009;6:699–710.
10. Papademetris X, Sinusas AJ, Dione DP, Constable RT, Duncan JS. Estimation of 3-D left ventricular deformation from medical images using biomechanical models. *IEEE Trans Med Imaging*. 2002;21:786–800.
11. Pengcheng S, Sinusas AJ, Constable RT, Ritman E, Duncan JS. Point-tracked quantitative analysis of left ventricular surface motion from 3-D image sequences. *IEEE Trans Med Imaging*. 2000;19:36–50.
12. Yan P, Sinusas A, Duncan J. Boundary element method-based regularization for recovering of LV deformation. *Med Image Anal*. 2007;11:540–554.
13. Schuleri KH, Centola M, George RT, Amado LC, Evers KS, Kitagawa K, Vavere AL, Evers R, Hare JM, Cox C, McVeigh ER, Lima JAC, Lardo AC. Characterization of peri-infarct zone heterogeneity by contrast-enhanced multidetector computed tomography: a comparison with magnetic resonance imaging. *J Am Coll Cardiol*. 2009;53:1699–1707.
14. Kellman P, Arai AE, McVeigh ER, Aletras AH. Phase-sensitive inversion recovery for detecting myocardial infarction using gadolinium-delayed hyperenhancement. *Magn Reson Med*. 2002;47:372–383.
15. Myronenko A, Song X. Point set registration: coherent point drift. *IEEE Trans Pattern Anal Mach Intell*. 2010;32:2262–2275.
16. Koenderink JJ, van Doorn AJ. Surface shape and curvature scales. *Image Vis Comput*. 1992;10:557–564.
17. Clarysse P, Friboulet D, Magnin IE. Tracking geometrical descriptors on 3-D deformable surfaces: application to the left-ventricular surface of the heart. *IEEE Trans Med Imaging*. 1997;16:392–404.
18. Cerqueira MD, Weissman NJ, Dilsizian V, Jacobs AK, Kaul S, Laskey WK, Pennell DJ, Rumberger JA, Ryan T, Verani MS. Standardized myocardial segmentation and nomenclature for tomographic imaging of the heart: a statement for healthcare professionals from the Cardiac Imaging Committee of the Council on Clinical Cardiology of the American Heart Association. *Circulation*. 2002;105:539–542.
19. Einstein AJ, Elliston CD, Arai AE, Chen MY, Mather R, Pearson GDN, DeLaPaz RL, Nickoloff E, Dutta A, Brenner DJ. Radiation dose from single-heartbeat coronary CT angiography performed with a 320-detector row volume scanner. *Radiology*. 2010;254:698–706.
20. Leipsic J, Nguyen G, Brown J, Sin D, Mayo JR. A prospective evaluation of dose reduction and image quality in chest CT using adaptive statistical iterative reconstruction. *Am J Roentgenol*. 2010;195:1095–1099.
21. Silva AC, Lawder HJ, Hara A, Kujak J, Pavlicek W. Innovations in CT dose reduction strategy: application of the adaptive statistical iterative reconstruction algorithm. *Am J Roentgenol*. 2010;194:191–199.
22. Renker M, Ramachandra A, Schoepf UJ, Raupach R, Apfaltrer P, Rowe GW, Vogt S, Flohr TG, Kerl JM, Bauer RW, Fink C, Henzler T. Iterative image reconstruction techniques: applications for cardiac Ct. *J Cardiovasc Comput Tomogr*. 2011;5:225–230.
23. Schaap M, Schilham A, Zuiderveld KJ, Prokop M, Vonken EJ, Niessen WJ. Fast noise reduction in computed tomography for improved 3-D visualization. *IEEE Trans Med Imaging*. 2008;27:1120–1129.
24. Borsdorf A, Raupach R, Flohr T, Hornegger J. Wavelet based noise reduction in CT-images using correlation analysis. *IEEE Trans Med Imaging*. 2008;27:1685–1703.
25. Ishizu T, Seo Y, Enomoto Y, Sugimori H, Yamamoto M, Machino T, Kawamura R, Aonuma K. Experimental validation of left ventricular transmural strain gradient with echocardiographic two-dimensional speckle tracking imaging. *Eur J Echocardiogr*. 2010;11:377–385.
26. Seo Y, Ishizu T, Enomoto Y, Sugimori H, Aonuma K. Endocardial surface area tracking for assessment of regional LV wall deformation with 3D speckle tracking imaging. *JACC Cardiovasc Imaging*. 2011;4:358–365.

### CLINICAL PERSPECTIVE

Determination of left ventricular regional function is important in the diagnosis and management of cardiomyopathy. We describe a novel, CT-based method, SQUEEZ (Stretch Quantifier for Endocardial Engraved Zones), that provides highly quantitative measures of regional myocardial function and can distinguish between infarcted and normally contracting myocardial regions with minimal user interaction and high resolution. This approach may have particular clinical value in assessing patients with dyssynchronous heart failure to better identify their candidacy for cardiac resynchronization therapy and may help to guide cardiac resynchronization therapy lead placement to the most appropriate myocardial location. Additionally, SQUEEZ may help to assess myocardial dysfunction in patients with myocardial ischemia, especially when used in tandem with CT coronary atherosclerosis and emerging CT regional blood flow assessment techniques.

**A New Method for Cardiac Computed Tomography Regional Function Assessment:  
Stretch Quantifier for Endocardial Engraved Zones (SQUEEZ)**  
Amir Pourmorteza, Karl H. Schuleri, Daniel A. Herzka, Albert C. Lardo and Elliot R. McVeigh

*Circ Cardiovasc Imaging*. 2012;5:243-250; originally published online February 16, 2012;  
doi: 10.1161/CIRCIMAGING.111.970061  
*Circulation: Cardiovascular Imaging* is published by the American Heart Association, 7272 Greenville Avenue,  
Dallas, TX 75231  
Copyright © 2012 American Heart Association, Inc. All rights reserved.  
Print ISSN: 1941-9651. Online ISSN: 1942-0080

The online version of this article, along with updated information and services, is located on the  
World Wide Web at:

<http://circimaging.ahajournals.org/content/5/2/243>

**Permissions:** Requests for permissions to reproduce figures, tables, or portions of articles originally published in *Circulation: Cardiovascular Imaging* can be obtained via RightsLink, a service of the Copyright Clearance Center, not the Editorial Office. Once the online version of the published article for which permission is being requested is located, click Request Permissions in the middle column of the Web page under Services. Further information about this process is available in the [Permissions and Rights Question and Answer](#) document.

**Reprints:** Information about reprints can be found online at:  
<http://www.lww.com/reprints>

**Subscriptions:** Information about subscribing to *Circulation: Cardiovascular Imaging* is online at:  
<http://circimaging.ahajournals.org/subscriptions/>